GW+DMFT approach for electronic structure calculations in real compounds

N.Zeyn **RRC "Kurchatov Institute", Moscow**

S. Savrasov **UCDavis, CA**

G. Kotliar **Rutgers University, NJ**

Supported by NSF,DOE

Contents

Gap in semiconductor. Comparison of LDA and GW with experiment

Semiconductor	LDA	FS GW	Exp
C	3.90	5.33	5.48
Si	0.52	0.90	1.17
Ge	0.05	0.62	0.74
LiH	2.57	5.1	4.94
MgO	5.2	8.3	7.8

Comparison of LDA and GW for (0,9) nanotube.

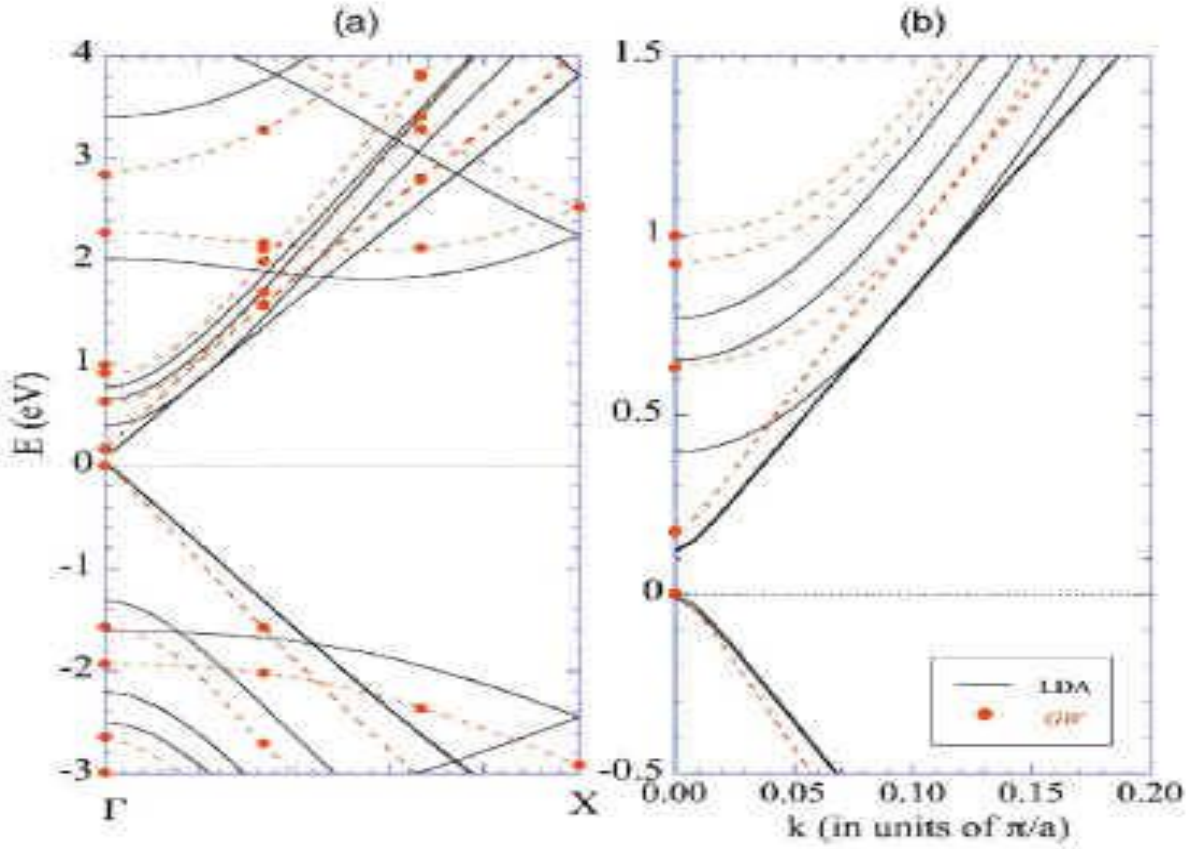

Gap changes from 0.08 eV to 0.17 eV

Intro. e-e interaction in homogeneous electron gas

Perturbation series can be resummed in terms of screened interaction W(ε). (Hedin 1965)

Series for thermodynamic energy (Luttiger-Ward functional) can be sketched as ln(G)–ΣG+Φ; Σ=δ Φ /δG

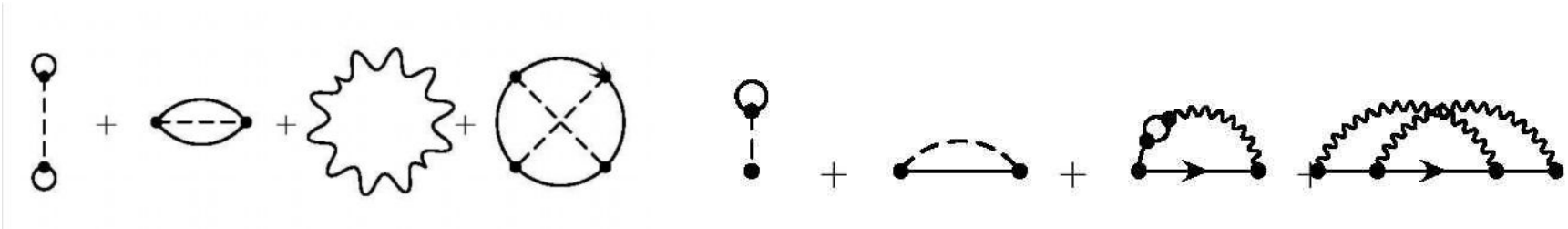

In perturbation theory first terms are

$$\varepsilon = \frac{1.11}{r_s^2} - \frac{0.458}{r_s} + \underbrace{0.0311 \ln r_s - 0.071}_{\text{GW diagram} \sim \text{Other Diagrams}} + 0.024 \ (a.u.)$$

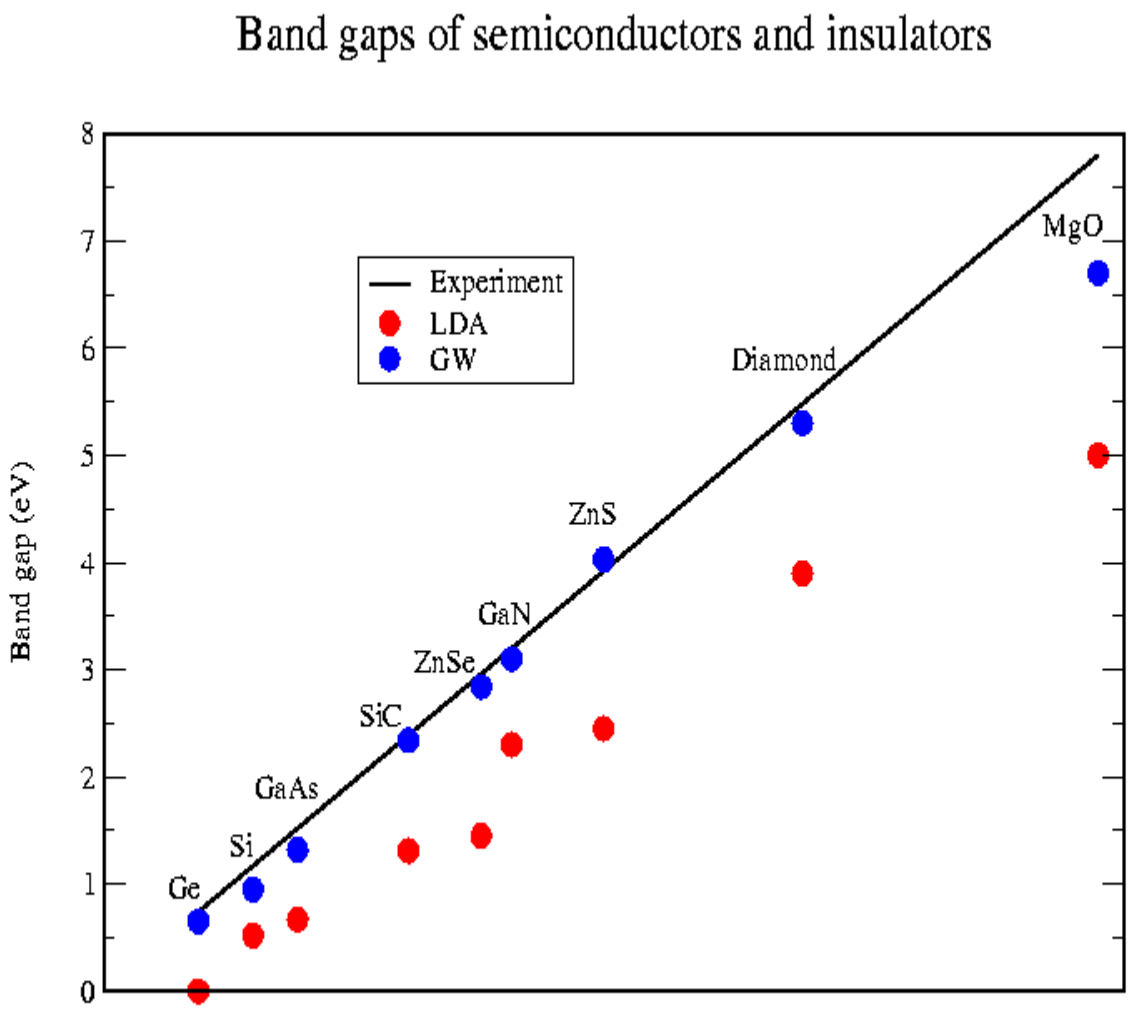
Band gaps of semiconductors and insulators
Band gap (eV)
0
1
2
3
4
5
6
7
8
Experiment
LDA
GW
Ge
Si
GaAs
SiC
ZnSe
GaN
ZnS
Diamond
MgO

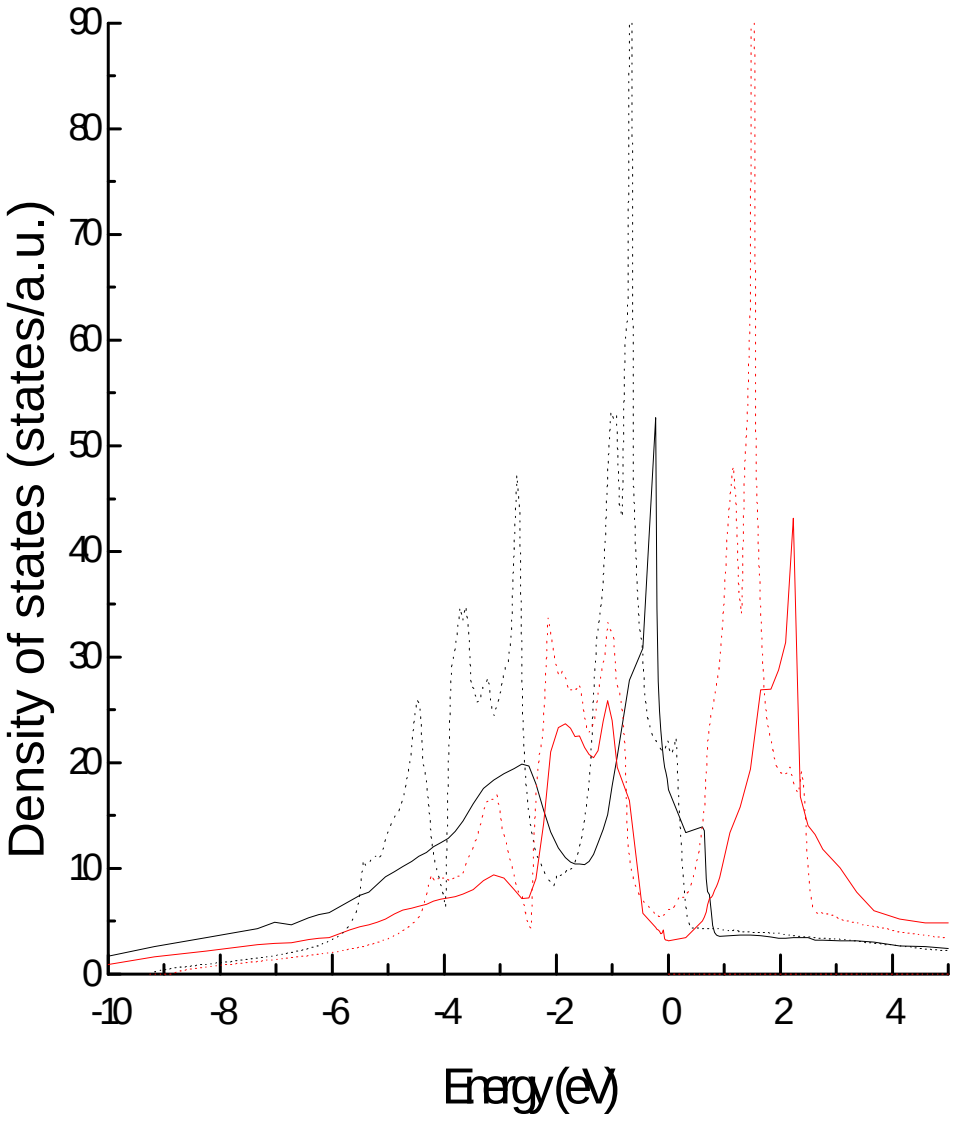
Density of states (states/a.u.)
Energy (eV)
0
10
20
30
40
50
60
70
80
90
-10
-8
-6
-4
-2
0
2
4

Local GW approach in 3d and 4d metals

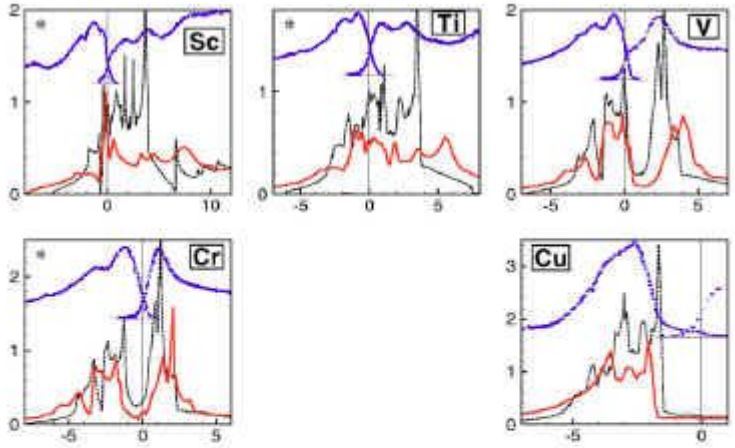

FIG. 1. (Color online) Spectral densities obtained in GW-OSA (solid red lines), LDA densities of states (dashed black lines), and experimental XPS and BIS spectra (dotted blue lines shifted up) for nonmagnetic 3*d* metals. Elements for which the crystal structure was not experimental are marked by a star in the upper left corner. In all graphs the *x* axis shows energy referenced from E_F in eV, and the *y* axis denotes the spectral density in eV^{-1} for the calculated curves.

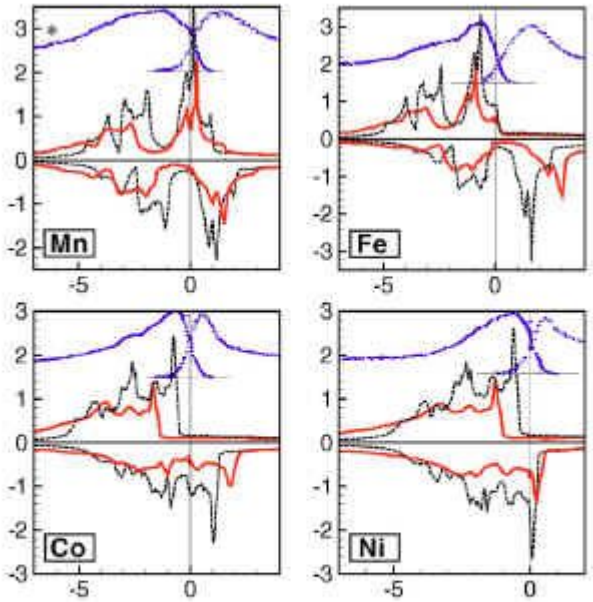

FIG. 2. (Color online) Same as in Fig. 1 but for magnetic 3*d* elements. The data for majority-spin and minority-spin electrons are plotted as positive and negative values, respectively.

Local GW approach in 3d and 4d metals

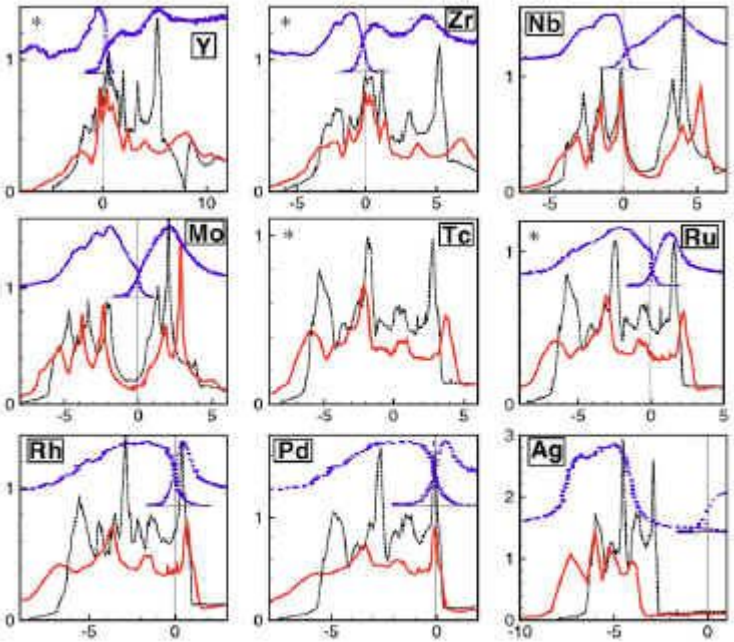

FIG. 3. (Color online) Same as in Fig. 1 but for 4*d* metals.

Variations of d-self-energy under iterations

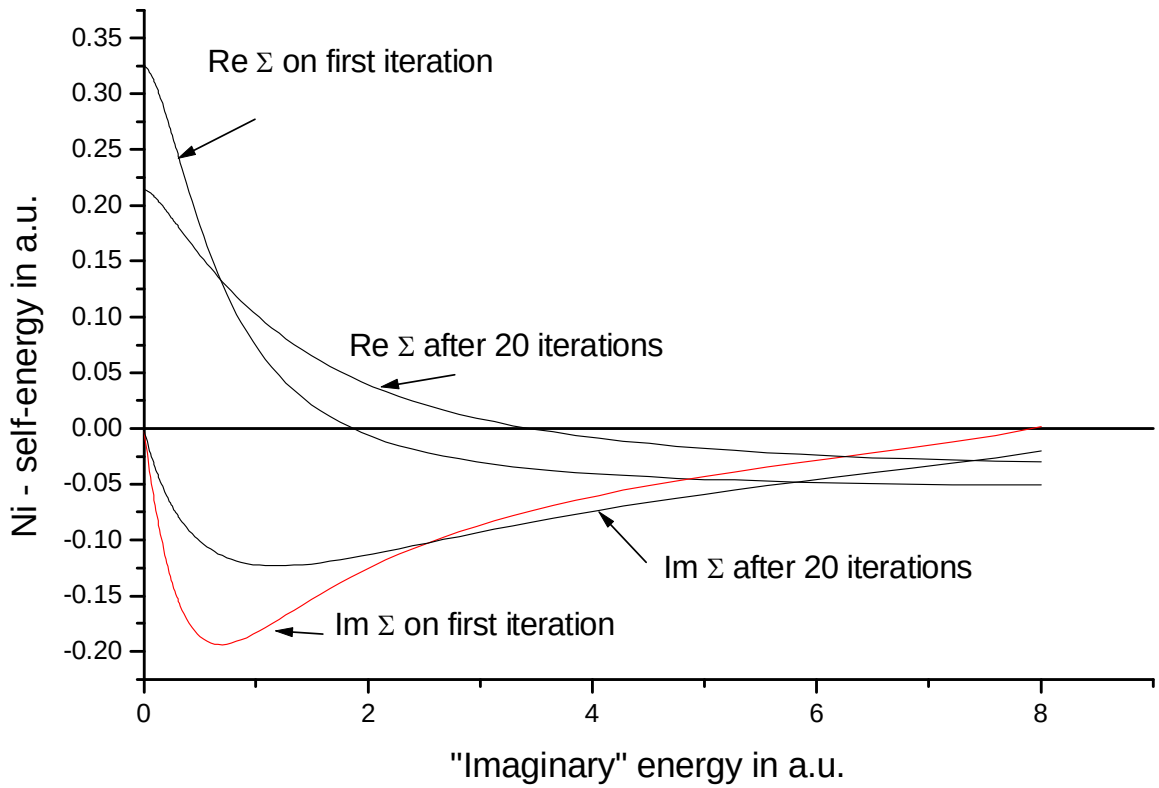

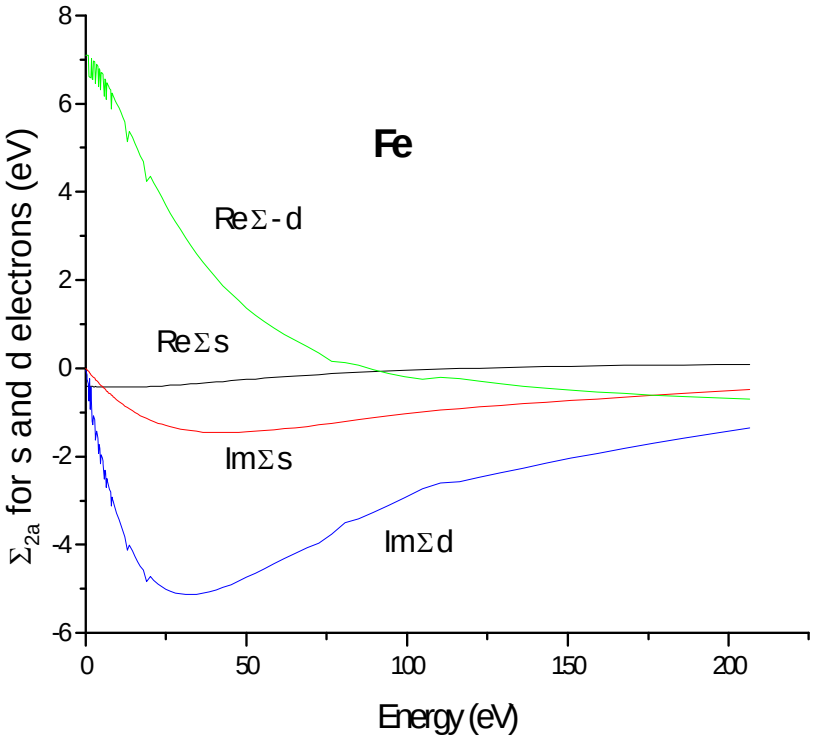
Fe
Re Σ - d
Re Σ s
Im Σ s
Im Σ d
Σ2a for s and d electrons (eV)
Energy (eV)
8
6
4
2
0
-2
-4
-6
0
50
100
150
200

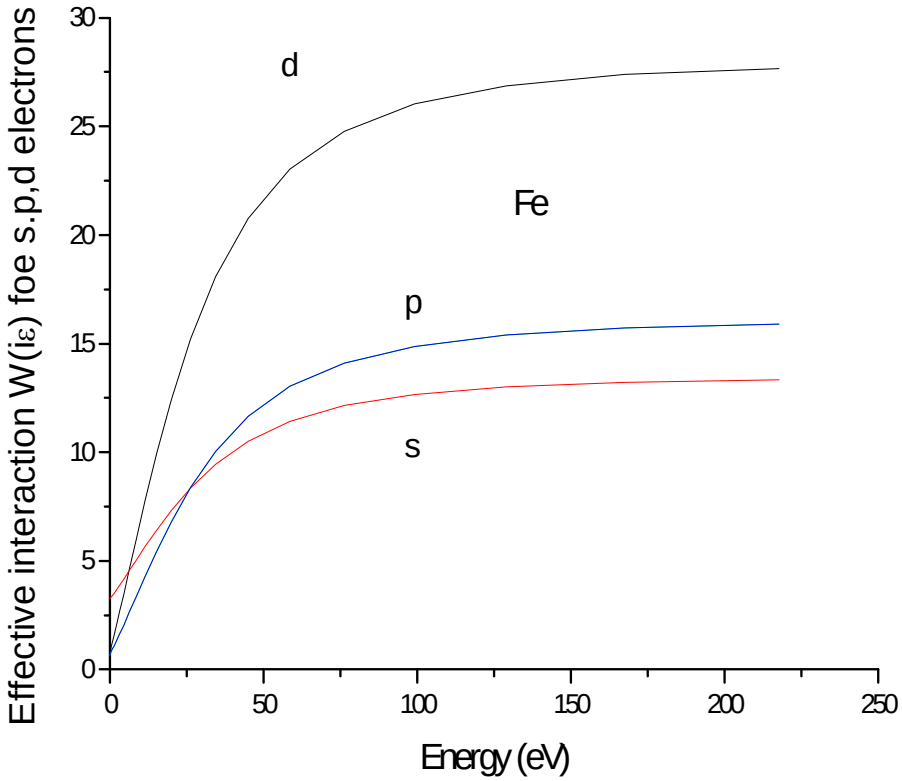
d
Fe
p
s
Effective interaction W(iε) foe s.p,d electrons
Energy (eV)
30
25
20
15
10
5
0
0
50
100
150
200
250

Convergence of correlational part of the self-energy Σ_{corr} in real space compared to bare Coulomb interaction in a.u. (1 a.u.= 27.2 eV) ***Test on transition metals***.

Self-energy

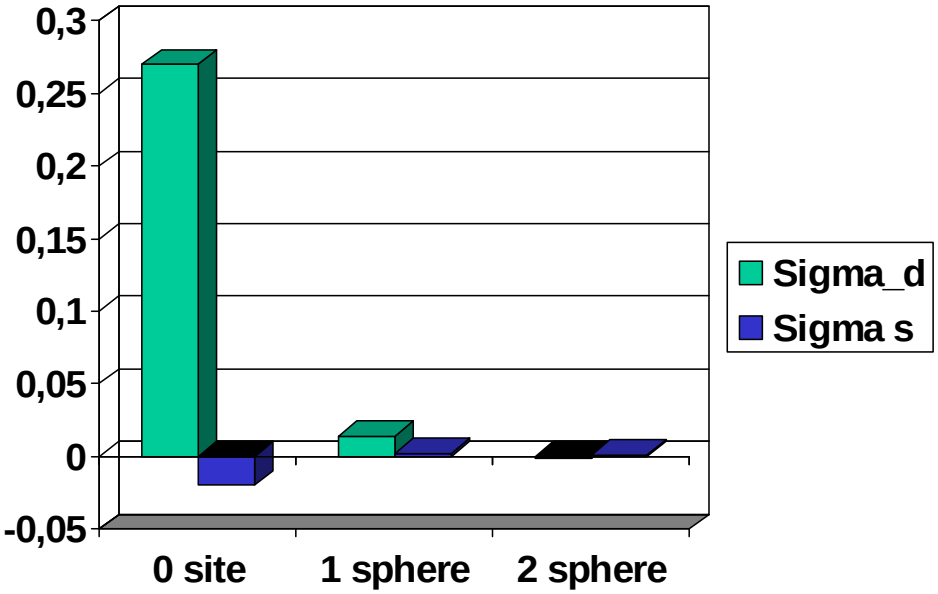

Matrix elements of bare Coulomb interaction

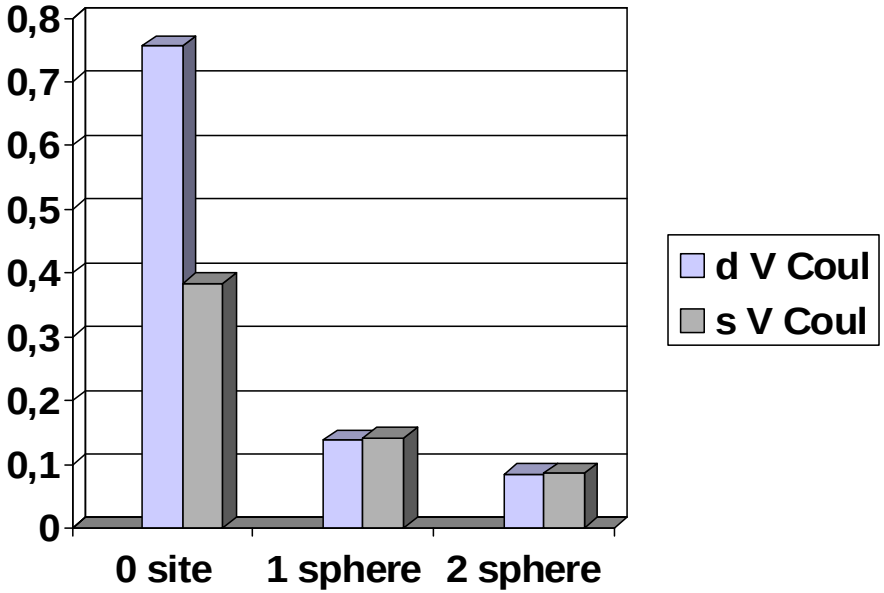

Convergence of correlational part of the self-energy Σ_{corr} compared to bare Coulomb interaction V (1 a.u.= 27.2 eV)

Test in simple metals

Self-energy

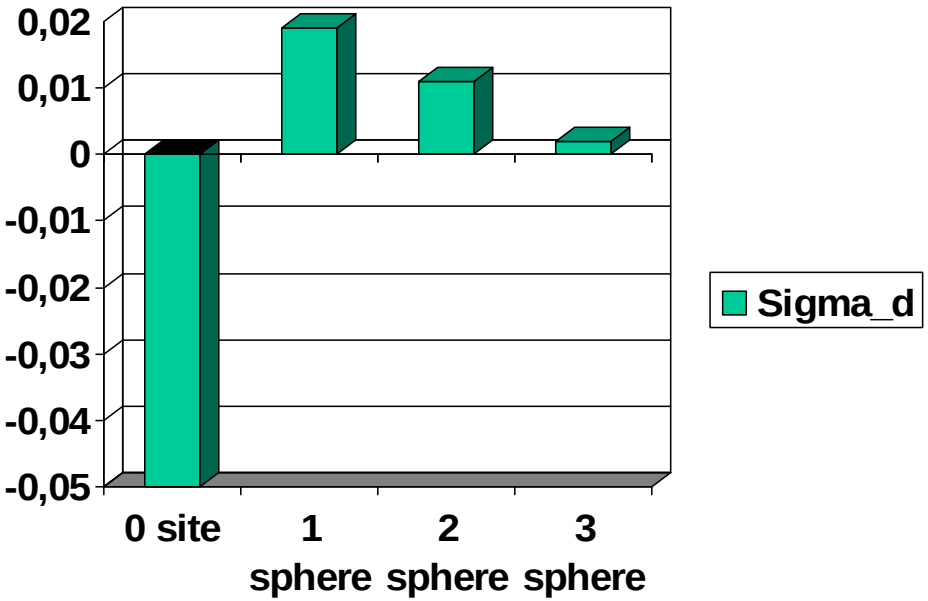

Matrix elements of bare Coulomb interaction

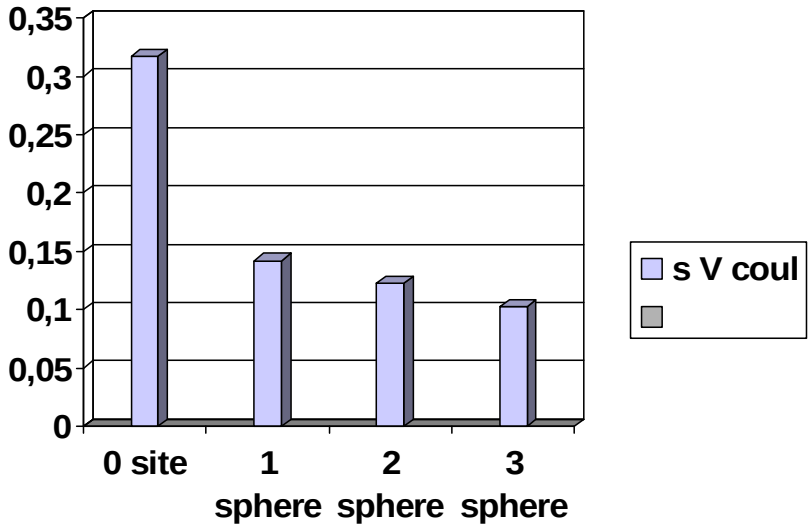

Σ_{exch}, Σ_{corr} for Si in a.u. (1 a.u.= 27.2 eV)

Exchange part of Self-energy

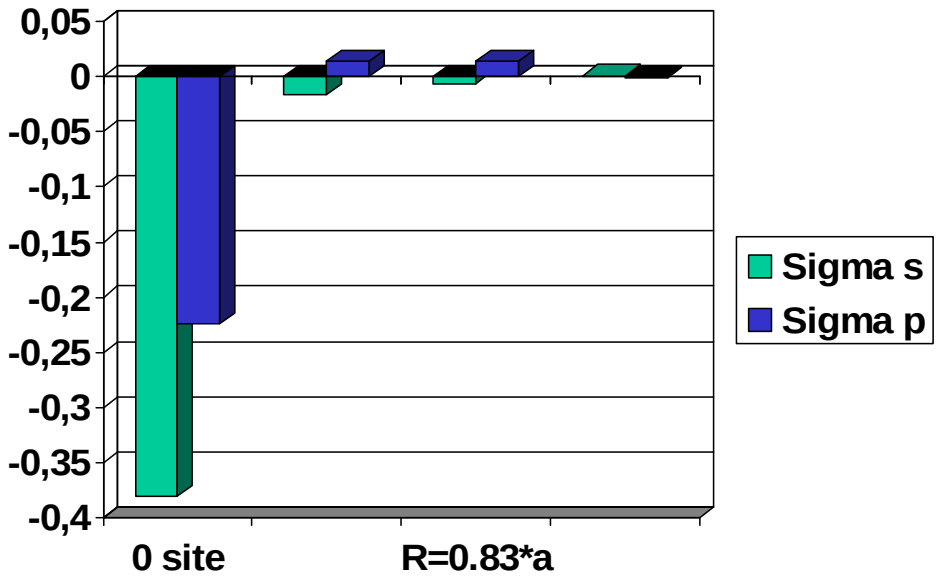

Correlational part of Self-energy

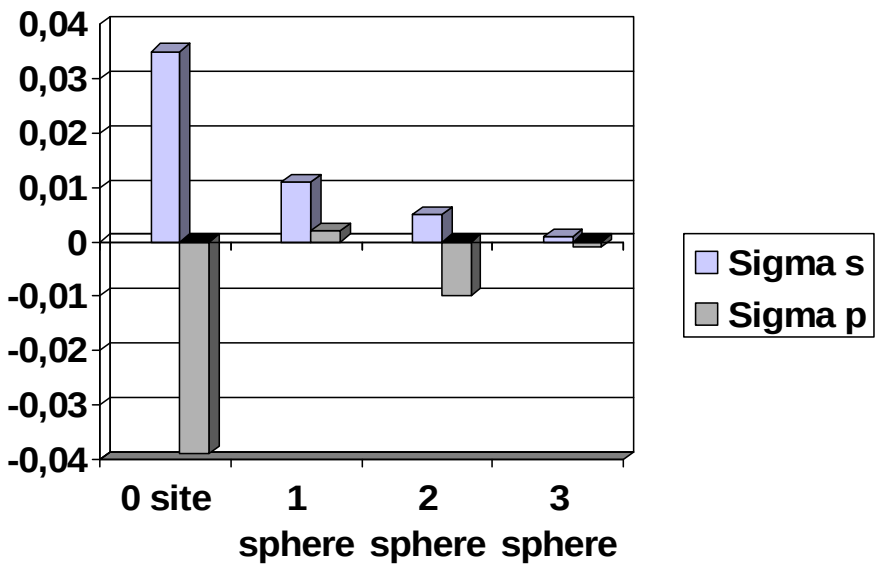

DMFT equations

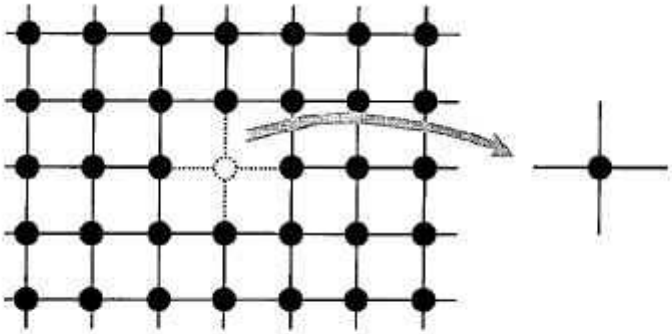

FIG. 1. Cavity created in the full lattice by removing a single site and its adjacent bonds.

$$\mathscr{S}_{\text{med}} = -\int d\tau \int d\tau' \sum_{\mathbf{k}\sigma} c^{+}_{\mathbf{k}\sigma}(\tau) G^{-1}_{\text{med}}(\mathbf{k}, \tau-\tau') c_{\mathbf{k}\sigma}(\tau'), \tag{53}$$

$$G_{\text{med}}(\mathbf{k}, i\omega_n)^{-1} = i\omega_n + \mu - \epsilon_{\mathbf{k}} - \Sigma(i\omega_n). \tag{54}$$

$$\mathscr{S}_{\text{emb}} = \mathscr{S}_{\text{med}} + U \int d\tau\, n_{o\uparrow} n_{o\downarrow} - \int d\tau \int d\tau' \sum_{\sigma} c^{+}_{o\sigma}(\tau) \Sigma(\tau-\tau') c_{o\sigma}(\tau').$$

$$S_{\text{eff}} = -\int d\tau \int d\tau' \sum_{\sigma} c^{+}_{o\sigma}(\tau) \mathscr{G}_0^{-1}(\tau-\tau') c_{o\sigma}(\tau') + U \int d\tau\, n_{o\uparrow} n_{o\downarrow}$$

DMFT equations

$$G_0^{-1} = i\omega_n - \varepsilon_0 - \Delta \qquad \frac{1}{i\omega_n - \varepsilon_0 - \Sigma(i\omega_n) - \Delta} = \sum_k \frac{1}{i\omega_n - \varepsilon_k - \Sigma(i\omega_n)} = G_{med}(R=0)$$

Connection with Anderson model

$$\Delta = \sum_i \frac{V_i^{\,2}}{i\omega_n - \varepsilon_i}$$

$$H_{\mathrm{AM}} = \sum_{l\sigma} \tilde{\varepsilon}_l a^+_{l\sigma} a_{l\sigma} + \sum_{l\sigma} V_l (a^+_{l\sigma} c_{o\sigma} + c^+_{o\sigma} a_{l\sigma})$$

$$- \mu \sum_{\sigma} c^+_{o\sigma} c_{o\sigma} + U n_{o\uparrow} n_{o\downarrow} .$$

Methods of DMFT equations solution

Approximate methods – Hubbard I, Gutzwiller, etc

Exact diagonalization method

Second order perturbation theory in Δ/U

Hirsh-Fye Monte-Carlo

Continuous Time Monte-Carlo with expansion in U (Rubtsov)

Continuous Time Monte-Carlo with expansion in Δ (Millis, Haule)

General Framework

Luttinger-Ward functional

$$\Gamma_0[G] = tr\ln G - tr[G/G_0 - 1] + \Phi[G]$$

Generalized Luttinger-Ward functional*

$$\Gamma[G,W] = tr\ln G - tr[G/G_0 - 1] - \frac{1}{2}tr\ln W + \frac{1}{2}tr[W/V - 1] + \boxed{\Psi[G,W]}$$

$$\frac{\delta\Gamma}{\delta G} = 0 \rightarrow G^{-1} = G_0^{-1} - \Sigma,$$

$$\frac{\delta\Gamma}{\delta W} = 0 \rightarrow W^{-1} = V^{-1} - P,$$

$$\boxed{\Sigma = \frac{\delta\Psi}{\delta G} \qquad P = 2\frac{\delta\Psi}{\delta W}}$$

*Almbladh, von Barth and van Leeuwen, *Int. J. Mod. Phys. B* 13, 535 (1999)
Chitra and Kotliar, *Phys. Rev. B* 63, 115110 (2001)

Approximation for Ψ

$$\Psi = \Psi_{GW}^{off-site}[G^{RR'}, W^{RR'}] + \Psi_{imp}^{on-site}[G^{RR}, W^{RR}]$$

$$\Psi_{GW}[G,W] = -\frac{1}{2} trGWG = -\frac{1}{2}$$

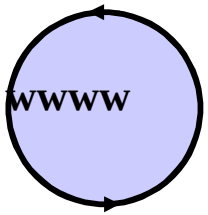

$$\frac{\delta\Psi}{\delta G} = \Sigma, \qquad \frac{\delta\Psi}{\delta W} = 2P$$

$$\Sigma(k, i\nu) = \Sigma_{GW}(k, i\nu) - \sum_k \Sigma_{GW}(k, i\nu) + \Sigma_{imp}(i\nu)$$

$$P(k, i\omega) = P_{GW}(k, i\omega) - \sum_k P_{GW}(k, i\omega) + P_{imp}(i\omega)$$

Метод GW+DMFT

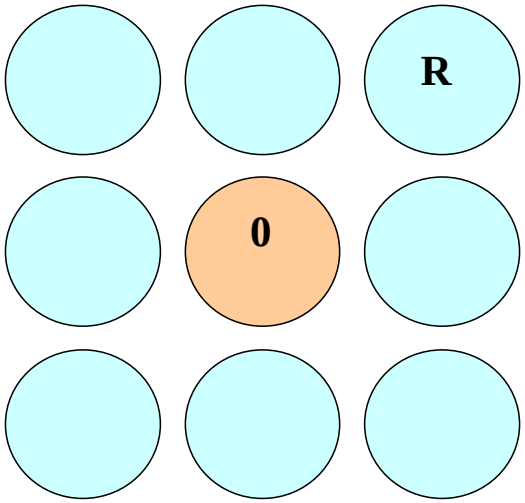

$$\Sigma_{00}(\omega) = \Sigma_{00}^{DMFT}(\omega)$$

$$\Sigma_{0R}(\omega) = \Sigma_{0R}^{GW}(\omega)$$

On-site self-energy Σ^{DMFT}.

Self-energy between sites Σ^{GW} .

Biermann Georges Liechtenstein…. PRL (2002)

Also can be reformulated using Luttinger-Word functional

GF+DMFT approach

7. We used LMTO-ASA method to build an appropriate basis

$$G^{-1}(\varepsilon_F)\Psi_k^{\nu}(r) = 0$$

Green function $(\varepsilon - H_0 - \Sigma)^{-1}$

$\Pi = -\Sigma(GG)$

$W = V/(1+V\,\Pi)$; $U = V(1+V\,\Pi_{rest})$

$\Sigma = GW + \Sigma_{solver}$

8. Matsubara Green functions. To obtain DOS we make analytical continuation of $\Sigma_{GW}(i\omega)$ by Pade – approximant procedure.

Direct Coulomb interaction

$$U^{l_1 l_2 l_3 l_4}_{m_1 m_2 m_3 m_4} = \sum_{lm} C^{lm}_{l_1 m_1 l_2 m_2} C^{lm}_{l_3 m_3 l_4 m_4} F_l$$

$$F_l = \int \phi_{l_1}(r)\phi_{l_2}(r) \frac{1}{2l+1} \frac{1}{r_>} \left(r_< / r_> \right)^l \phi_{l_3}(r')\phi_{l_4}(r') dr dr'$$

For homogeneous sphere with radius R

$$F_0 = \rho^2 2 \int_0^R r^2 dr \frac{1}{r} \int_0^r r'^2 dr' = \frac{6}{5R} (a.u.) \qquad \rho^{-1} = \frac{R^3}{3}$$

Pure Coulomb interaction

HEG	ss	pp	dd
ss	0.430	0.417	0.406
pp	0.417	0.409	0.400
dd	0.406	0.400	0.394

F_2=0.030 F_4=0.009

Ni –F_0	ss	pp	dd
ss	0.470	0.466	0.549
pp	0.466	0.462	0.543
dd	0.549	0.543	0.940

F2=0.019 F4=0.003

Pure Coulomb interaction

Ce	ss	pp	dd	ff
ss	0.327	0.319	0.345	0.401
pp		0.313	0.333	0.368
dd			0.379	0.457
ff				0.846

Constrained LDA method
Dederichs 1984, Gunnarson 1989, Anisimov 1991

$$U = \frac{\delta^2 E(N_d)}{\delta N_d^2}$$

$$E(N_d) = \min\{E(n) + v_d \int d^3 r (n_d - N_d)\}$$

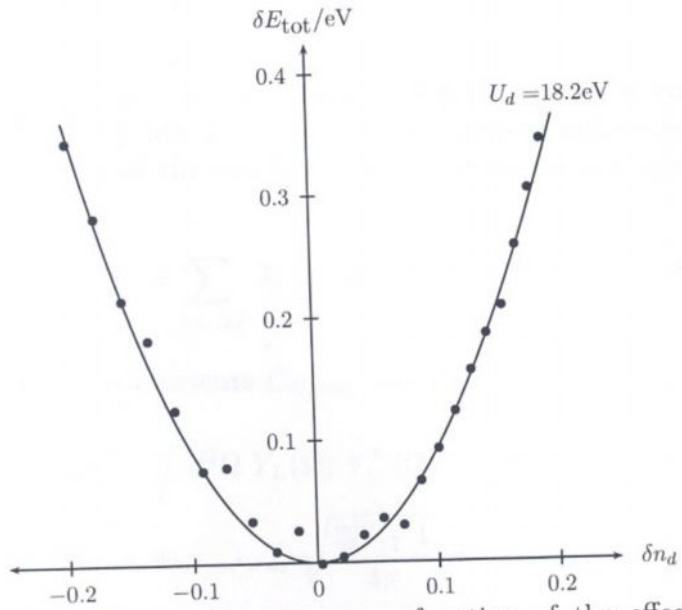

FIG. 8. The total energy as a function of the effective change in d charge. The line is a quadratic fit.

GW approach to U

Effective Hubbard model

$$\int D\varphi_s^+ D\varphi_s \exp(-\int d\tau H(\tau,\varphi_s,\varphi_d)) = \exp(-\int d\tau H_{eff}(\tau,\varphi_d))$$

$$H_{dd}^2 = H_{dd}^0 - \frac{V_{sd}^2}{i\omega - \varepsilon_s^k} + \Sigma(G_{ss})$$

$$U = V_{dd} + \Gamma(G_{ss})$$

$$\Gamma \approx W(\Pi_{ss})$$

$$\Gamma_6, \quad \Gamma_8, \ldots$$

$$
\begin{aligned}
W &= [1 - vP]^{-1} v \\
&= [1 - vP_r - vP_d]^{-1} v \\
&= [(1 - vP_r)\{1 - (1 - vP_r)^{-1} vP_d\}]^{-1} v \\
&= \{1 - (1 - vP_r)^{-1} vP_d\}^{-1} (1 - vP_r)^{-1} v \\
&= [1 - W_r P_d]^{-1} W_r
\end{aligned}
$$

$$
W_r(\omega) = [1 - vP_r(\omega)]^{-1} v
$$

$$
W_r(\omega) \to U(\omega)
$$

Energy-dependent effective interaction between the 3d electrons

$$
\begin{aligned}
S = \iint d\tau d\tau' \Big[& \sum c_n^+(\tau) G_{nn'}^{-1}(\tau - \tau') c_{n'}(\tau') \\
& + \frac{1}{2} \sum : c_n^+(\tau) c_{n'}(\tau) : U_{nn',mm'}(\tau - \tau') : c_m^+(\tau') c_{m'}(\tau') : \Big]
\end{aligned}
$$

On-site U for the 3d series

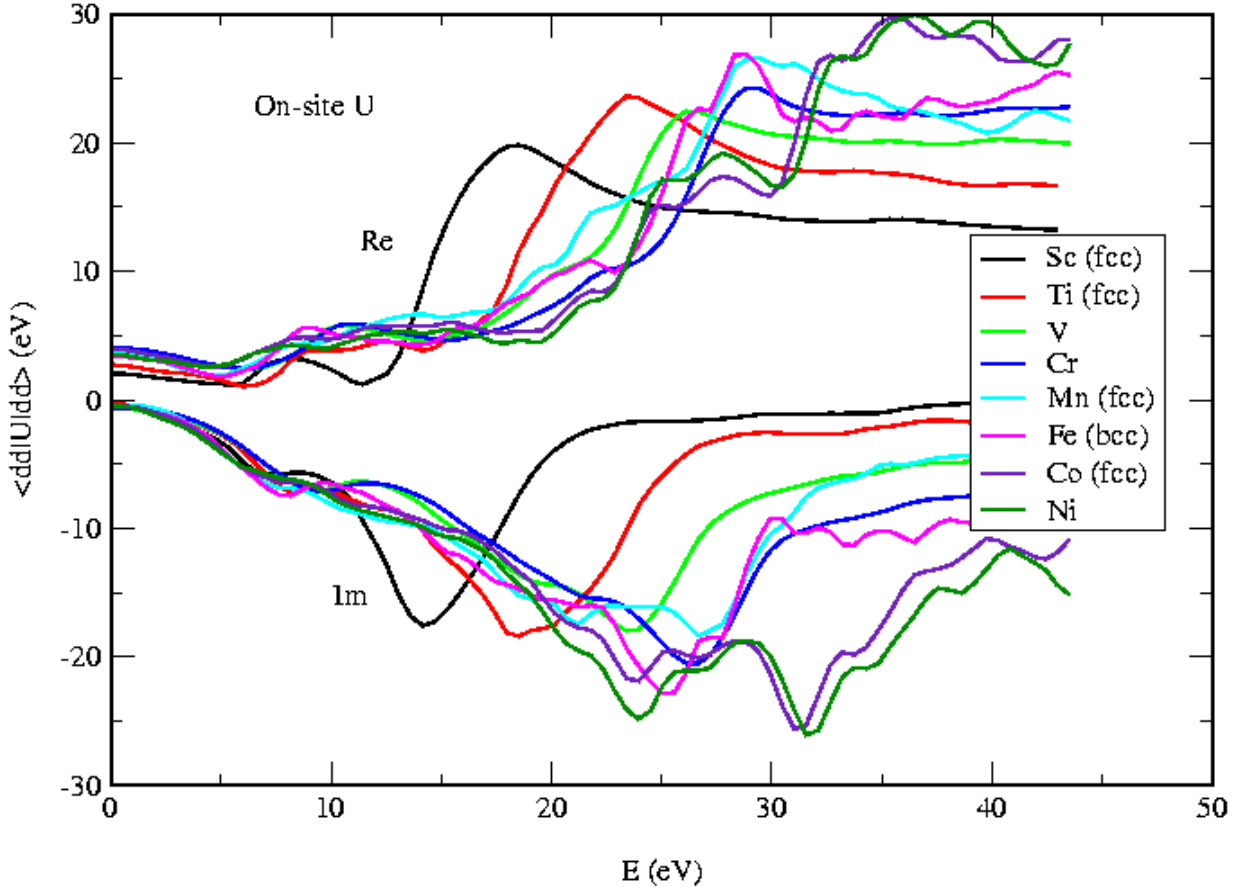

$$\mathrm{Re}\,U(\omega) = v + \int d\omega' \frac{|\,\mathrm{Im}\,U(\omega')\,|}{\omega - \omega'}$$

On-site U(0) is between 2-4 eV

$$\mathrm{Re}\,U(0) \approx v - \frac{c}{\omega_p}$$

Nearest-neighbour U for the 3d series

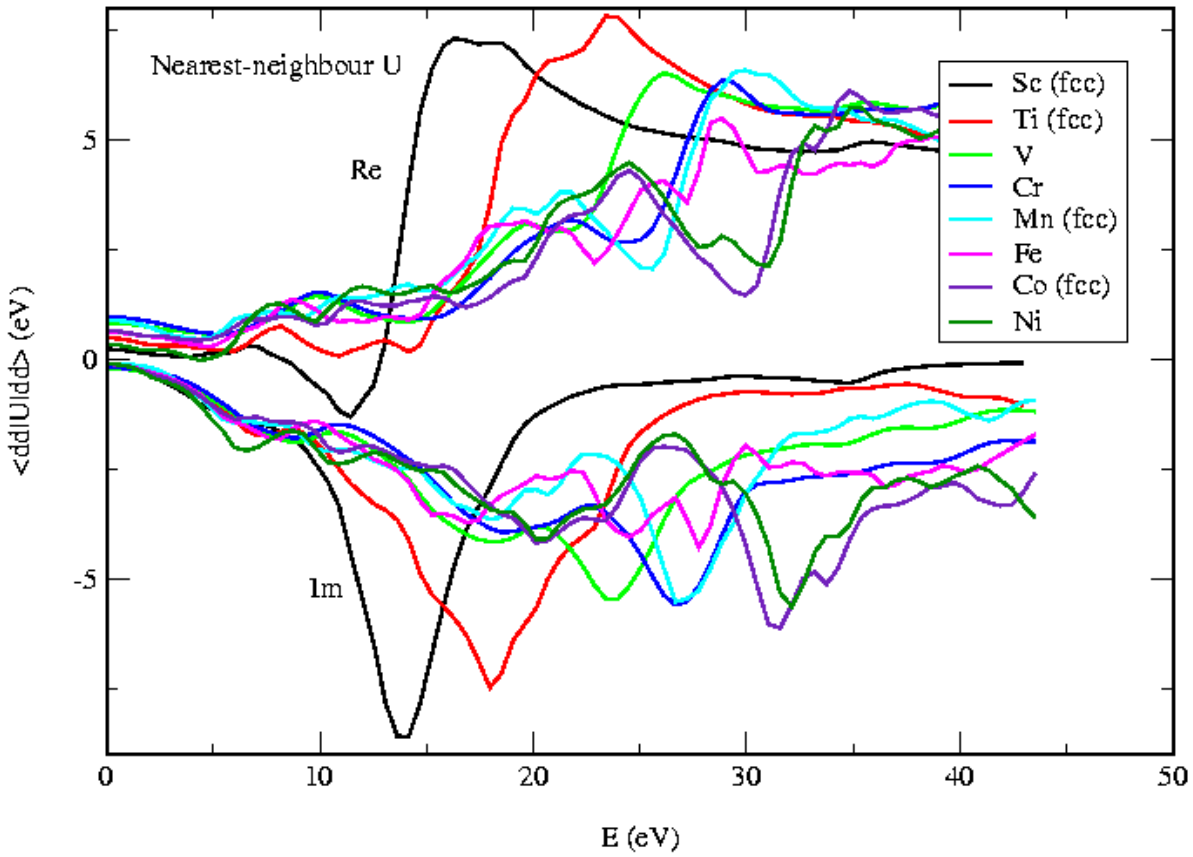

Nearest-neighbour U(0) is between 0.2-1.0 eV

Static Hubbard U for the 3d series

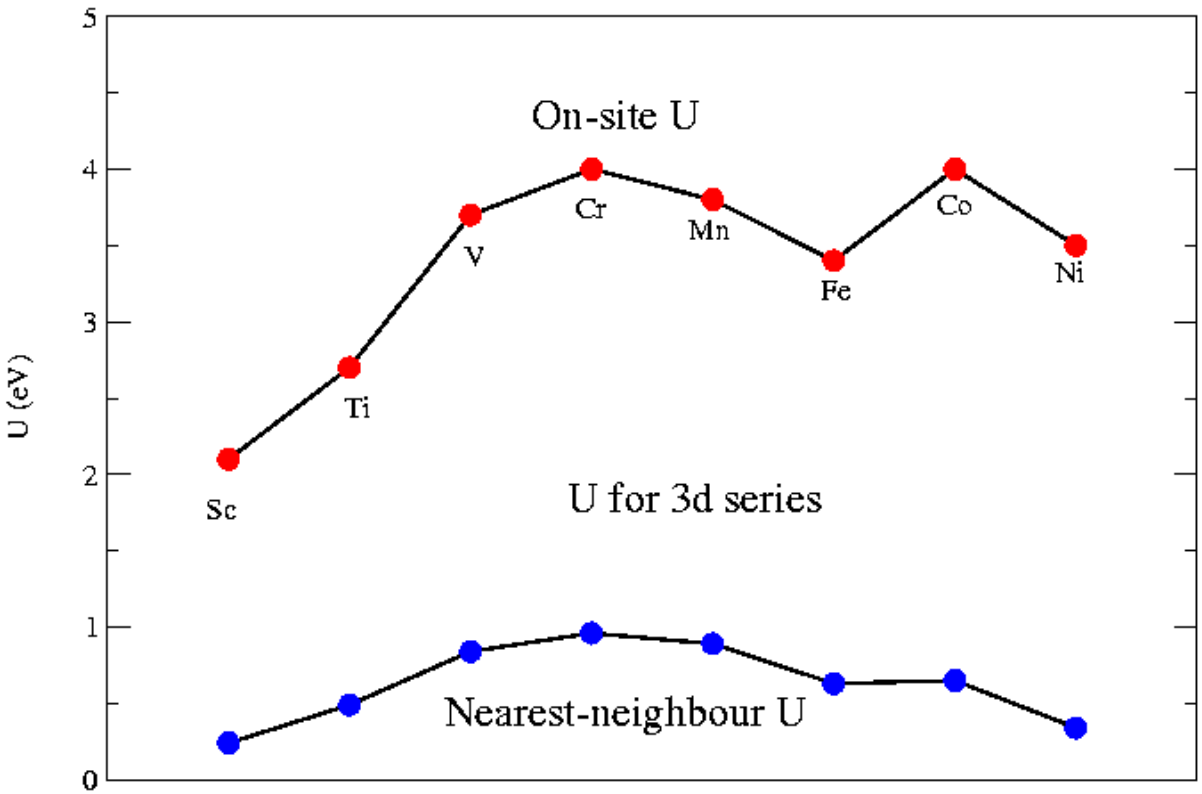

Energy dependence of interaction in NiO

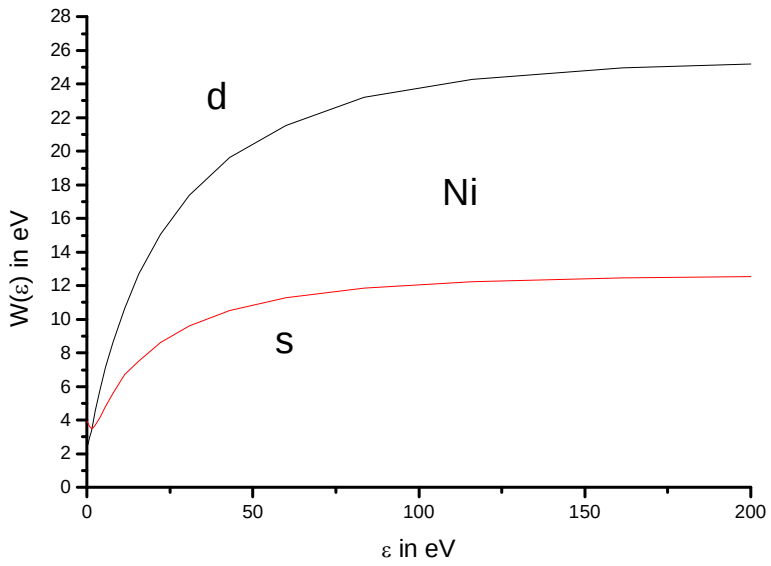

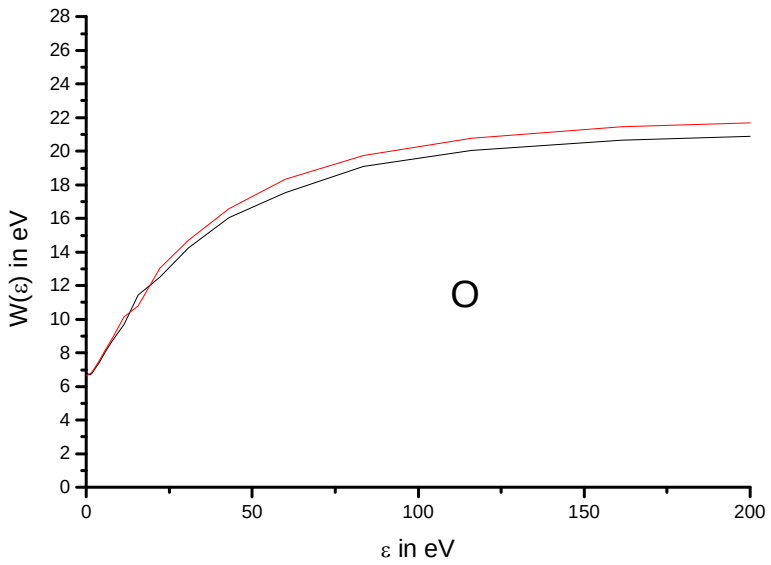

Antiferromagnetic NiO: LDA and GW calculations

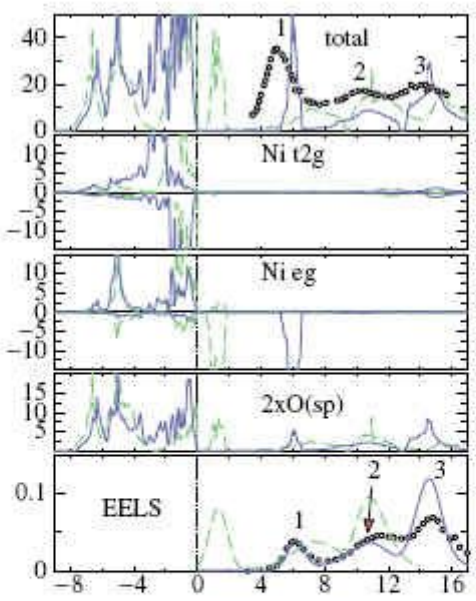

FIG. 3 (color online). DOS and electron-energy-loss spectroscopy (EELS) of NiO. Solid lines: SCGW data; dash-dotted lines: LDA data. Top panel: total DOS, together with BIS data of Ref. [14] (circles). Panels 2 and 3 show the Ni t_{2g} and e_g partial DOS, with positive DOS showing majority spin and negative showing minority spin. Panel 4 shows the O sp partial DOS; panel 5 compares the calculated and measured [17] EELS spectra from the O $1s$ level.

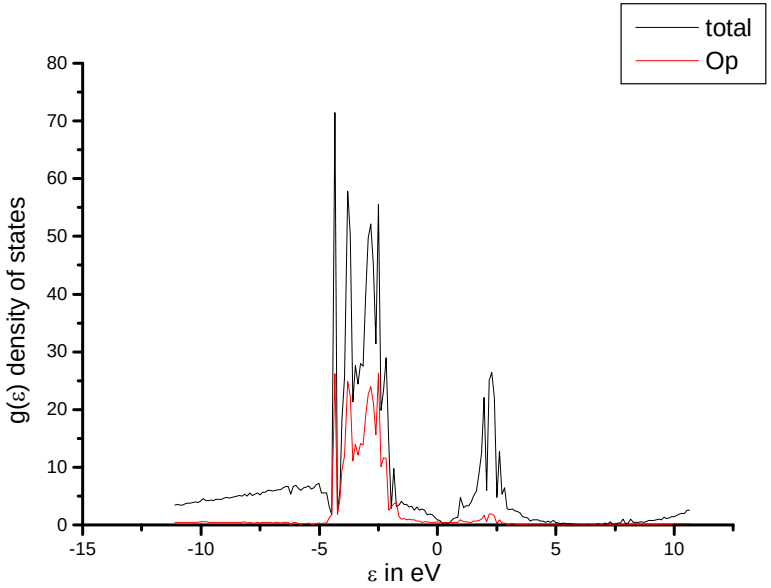

Faleev, Schilfgaarde, Kotani PRL 93 (2004)

Schematic levels in Mott insulator NiO

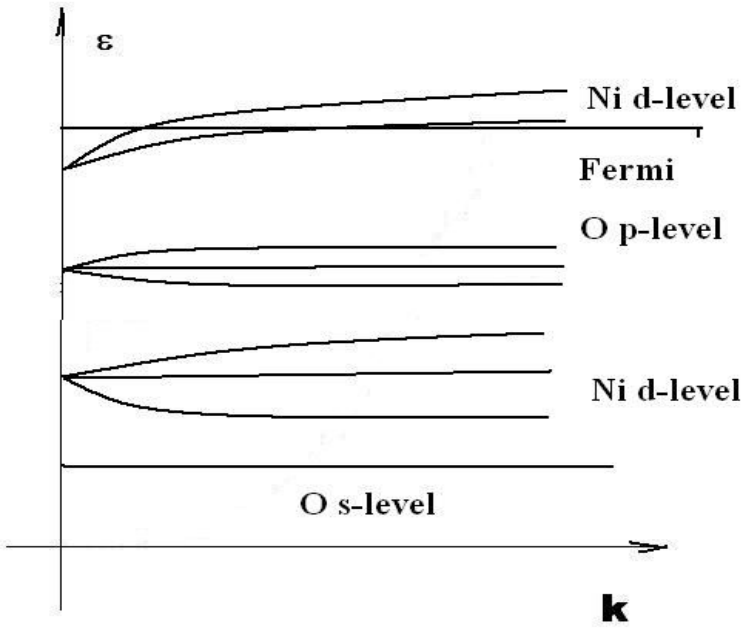

Density of states (DOS)in paramagnetic NiO
Left: DF approach -> металл(DOS at Fermi)
Right : GW+DMFT->insulator (gap)

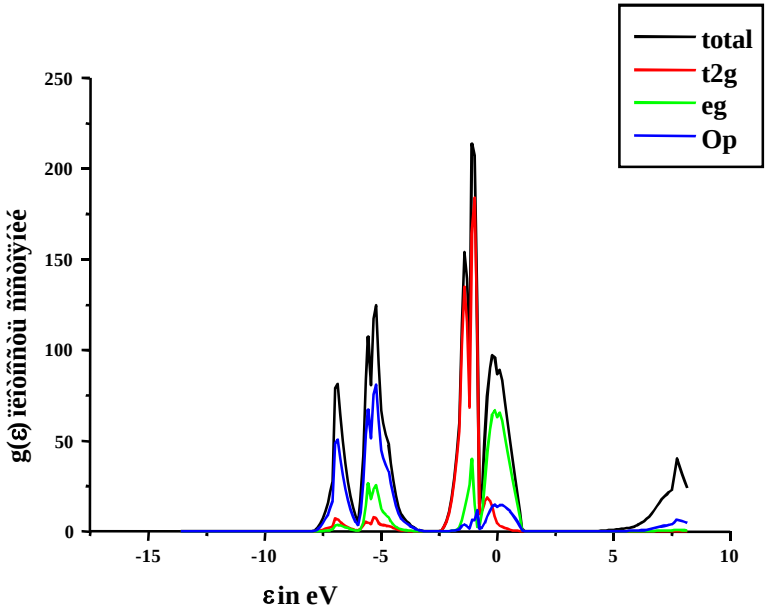

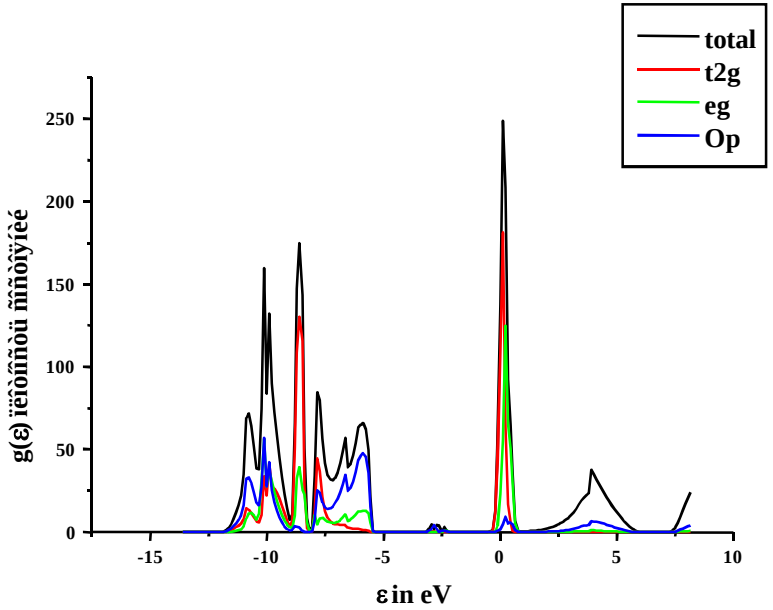

In experiment NiO is an insulator with gap 4.5 eV

Hubbard and charge-transfer models

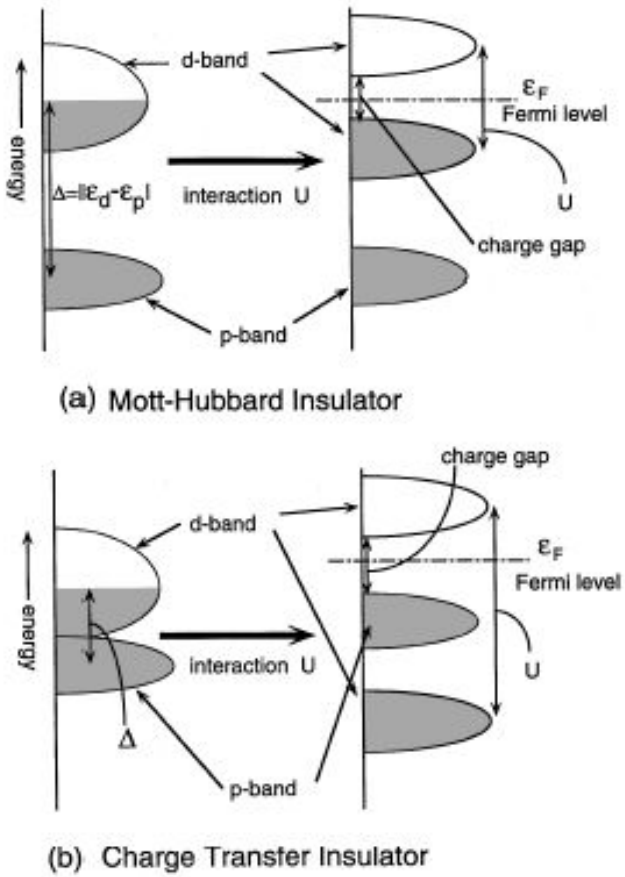

FIG. 5. Schematic illustration of energy levels for (a) a Mott-Hubbard insulator and (b) a charge-transfer insulator generated by the d-site interaction effect.

Experiment in NiO

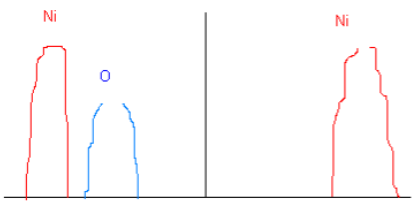

Charge-transfer model

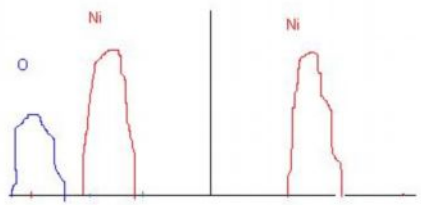

Hubbard model

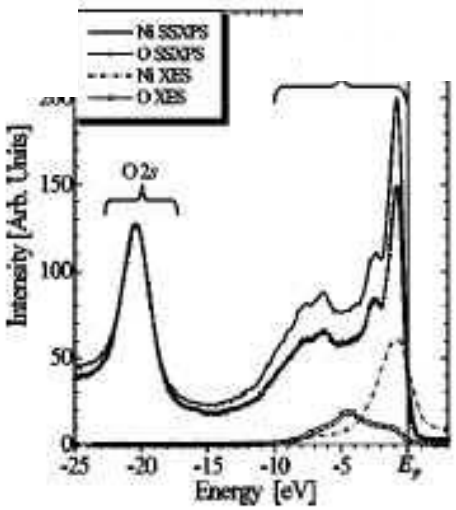

PRB 71 (2005)

FIG. 4. A comparison of valence state measurements using XES and SSXPS experimental techniques. The spectra show comparable peak structure just below the valence band maximum (0 eV), and the Ni and O SSXPS spectra show nearly complete hybridization.

LDA+EX-DIAG в NiO
Savrasov et.al PRL (2008)

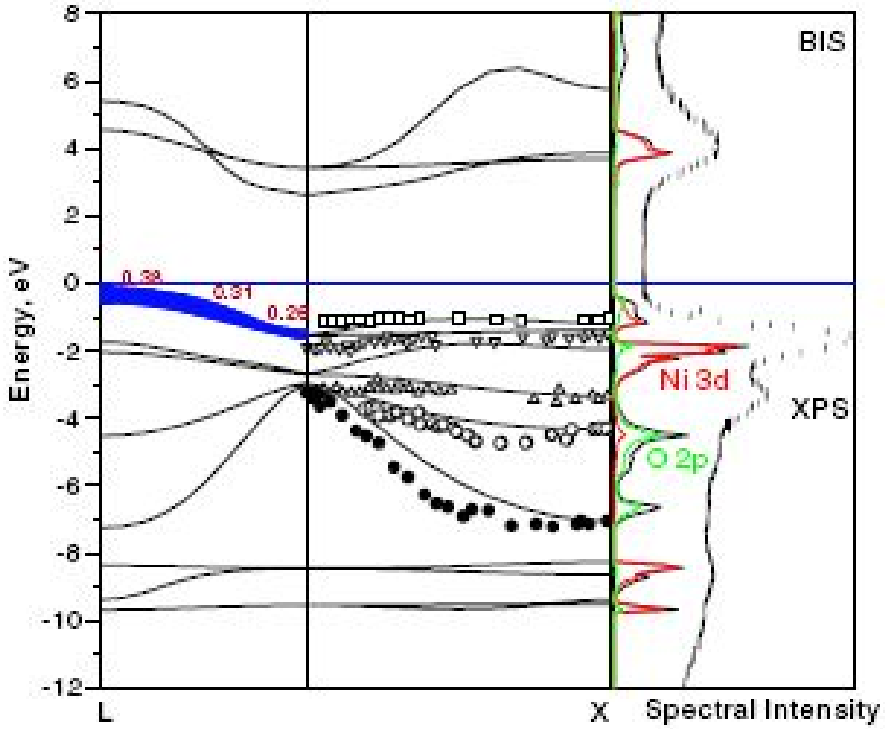

FIG. 2 (color online). Comparison between calculated quasi-particle dispersions using LDA + DMFT and the photoemission data [5,23] for paramagnetic state of NiO. The solid linewidth and the numbers show the oxygen content and the amount of electrons in the ZR band.

Conclusion

- 1. **Self-consistent** GW method was implemented for 3D and 1D crystal structures.
- 2. R-space convergence was investigated.
- 3. GW+DMFT approach was applied for electronic structure calculations in Mott insulator – paramagnetic NiO.
- 4. GW+DMFT with Monte-Carlo solver - in progress.

Self-consistency loop

Impurity: given Weiss field $\mathcal{G}$ and U

$$\Sigma_{imp} = \mathcal{G}^{-1} - G_{imp}^{-1}$$

$$W_{imp} = U - U\chi_{imp}U$$

$$P_{imp} = U^{-1} - W_{imp}^{-1}$$

New Weiss field $\mathcal{G}$ and U

$$\mathcal{G}^{-1} = G_{loc}^{-1} + \Sigma_{imp}$$

$$U^{-1} = W_{loc}^{-1} + P_{imp}$$

Combine Σ_{GW} and Σ_{imp}

$$\Sigma(k) = \Sigma_{GW}(k) - \sum_q \Sigma_{GW}(q) + \Sigma_{imp}$$

$$P(k) = P_{GW}(k) - \sum_q P_{GW}(q) + P_{imp}$$

Check self-consistency: G_{loc}=G_{imp}? W_{loc}=W_{imp}?

$$G_{loc} = \sum_k [G_0^{-1}(k) - \Sigma(k)]^{-1}$$

$$W_{loc} = \sum_k [V^{-1}(k) - P(k)]^{-1}$$

Self-Consistency Conditions

$$G_{loc} = \sum_k [G_0^{-1}(k) - \Sigma(k)]^{-1} = G_{imp}$$

$$W_{loc} = \sum_k [V^{-1}(k) - P(k)]^{-1} = W_{imp}$$

$$G_{imp}(\tau) \equiv - < Tc_0(\tau) c_0^+(0) >_{S_{eff}}$$

$$W_{imp} = U - U \chi_{imp} U$$

$$\sum_k \Sigma_{GW}(k,\tau) = -G_{imp}(\tau) W_{imp}(\tau)$$

The Hubbard U is screened within the impurity model such that the screened U is equal to the local W

Exact diagonalization method

States

$$| c_i^+ c_j^+ c_k^+ \ldots . d_p^+ d_q^+ \ldots . >$$

$$H = \varepsilon_p \sum_i c_{p_i}^+ c_{p_i} + \sum_i V_i (c_{p_i}^+ d_{m_i} + d_{m_i}^+ c_{p_i}) + \sum_i \varepsilon_{m_i} d_m^+ d_{m_i} +$$

$$U n_d n_d + \sum_{L=2,4} F^L G_{m_1 m_4}^L G_{m_3 m_2}^L d_{m_1}^+ d_{m_2}^+ d_{m_3} d_{m_4}$$

Second order perturbation theory

$$
\begin{aligned}
G^2_{\alpha\beta}(i\omega) = \sum_{0,1,2,3,\gamma\delta} & (F^\alpha)_{01}(F^{\gamma\dagger})_{12}(F^\delta)_{23}(F^{\beta\dagger})_{30}\left[\frac{\mathcal{R}_{\gamma\delta}(E_1,E_2)}{E_{13}}\frac{1}{i\omega-E_{10}}+\frac{\mathcal{R}_{\gamma\delta}(E_3,E_2)}{E_{31}}\frac{1}{i\omega-E_{30}}+\frac{\mathcal{Q}_{\gamma\delta}(i\omega,E_0,E_2)}{(i\omega-E_{30})(i\omega-E_{10})}\right] \\
& + (F^\alpha)_{01}(F^\delta)_{12}(F^{\gamma\dagger})_{23}(F^{\beta\dagger})_{30}\left[\frac{\mathcal{R}_{\gamma\delta}(E_2,E_1)}{E_{13}}\frac{1}{i\omega-E_{10}}+\frac{\mathcal{R}_{\gamma\delta}(E_2,E_3)}{E_{31}}\frac{1}{i\omega-E_{30}}-\frac{\mathcal{Q}_{\gamma\delta}(-i\omega,E_2,E_0)}{(i\omega-E_{30})(i\omega-E_{10})}\right] \\
& + (F^{\gamma\dagger})_{01}(F^\delta)_{12}(F^\alpha)_{23}(F^{\beta\dagger})_{30}\left[\frac{\mathcal{R}_{\gamma\delta}(E_2,E_1)}{E_{20}}\frac{1}{i\omega-E_{32}}+\frac{\mathcal{R}_{\gamma\delta}(E_0,E_1)}{E_{02}}\frac{1}{i\omega-E_{30}}-\frac{\mathcal{Q}_{\gamma\delta}(-i\omega,E_3,E_1)}{(i\omega-E_{30})(i\omega-E_{32})}\right] \\
& + (F^\delta)_{01}(F^{\gamma\dagger})_{12}(F^\alpha)_{23}(F^{\beta\dagger})_{30}\left[\frac{\mathcal{R}_{\gamma\delta}(E_1,E_2)}{E_{20}}\frac{1}{i\omega-E_{32}}+\frac{\mathcal{R}_{\gamma\delta}(E_1,E_0)}{E_{02}}\frac{1}{i\omega-E_{30}}+\frac{\mathcal{Q}_{\gamma\delta}(i\omega,E_1,E_3)}{(i\omega-E_{30})(i\omega-E_{32})}\right] \\
& + (F^\delta)_{01}(F^\alpha)_{12}(F^{\gamma\dagger})_{23}(F^{\beta\dagger})_{30}\frac{1}{(i\omega-E_{21})(i\omega-E_{30})}[\mathcal{R}_{\gamma\delta}(E_2,E_3)-\mathcal{R}_{\gamma\delta}(E_1,E_0)+\mathcal{Q}_{\gamma\delta}(i\omega,E_1,E_3)-\mathcal{Q}_{\gamma\delta}(-i\omega,E_2,E_0)] \\
& + (F^{\gamma\dagger})_{01}(F^\alpha)_{12}(F^\delta)_{23}(F^{\beta\dagger})_{30}\frac{1}{(i\omega-E_{21})(i\omega-E_{30})}[\mathcal{R}_{\gamma\delta}(E_3,E_2)-\mathcal{R}_{\gamma\delta}(E_0,E_1)+\mathcal{Q}_{\gamma\delta}(i\omega,E_0,E_2)-\mathcal{Q}_{\gamma\delta}(-i\omega,E_3,E_1)],
\end{aligned}
\tag{16}
$$

where we used the notation $E_{ij}=E_i-E_j$ and the functions $\mathcal{R}_{\gamma\delta}$ and $\mathcal{Q}_{\gamma\delta}$ are

$$
\mathcal{R}_{\gamma\delta}(E_1,E_2) \equiv (X_1+X_2)T\sum_{i\omega'}\frac{\Delta_{\gamma\delta}(i\omega')}{i\omega'-E_{12}},
$$

$$
\mathcal{Q}_{\gamma\delta}(i\omega,E_1,E_2) \equiv (X_1-X_2)T\sum_{i\omega'}\frac{\Delta_{\gamma\delta}(i\omega')}{i\omega'-i\omega-E_{12}}, \tag{17}
$$

condition described in Ref 1, this method can be used as a very efficient impurity solver in the DMFT study of the multiorbital systems with very complicated local interactions.

III. BENCHMARK

To test this impurity solver, we calculated the Green's function for the two-band Hubbard model at half filling and compared it with the results obtained by the QMC solver. We

Effective interaction among electrons in a narrow band

Suppose the bandstructure of a given solid can be well separated into a narrow band near the Fermi level and the rest, e.g., transition metals or 4f metals.

We write the total polarisation as

$$P = P_d + P_r$$

$$P_d = 3d \rightarrow 3d$$ **transitions only**

M. Springer and Aryasetiavan, PRB 57, 4364 (1998)
T. Kotani, J. Phys. Cond. Matt. 12, 2413 (2000)
Aryasetiavan, Imada, Georges, Kotliar, Biermann, Lichtenstein, PRB 70, 195104 (2004)

Диаграммное разложение по гибридизации Δ
взвешивание диаграмм по Метрополису
Millis et al PRB (2006)
K. Haule PRB (2007)

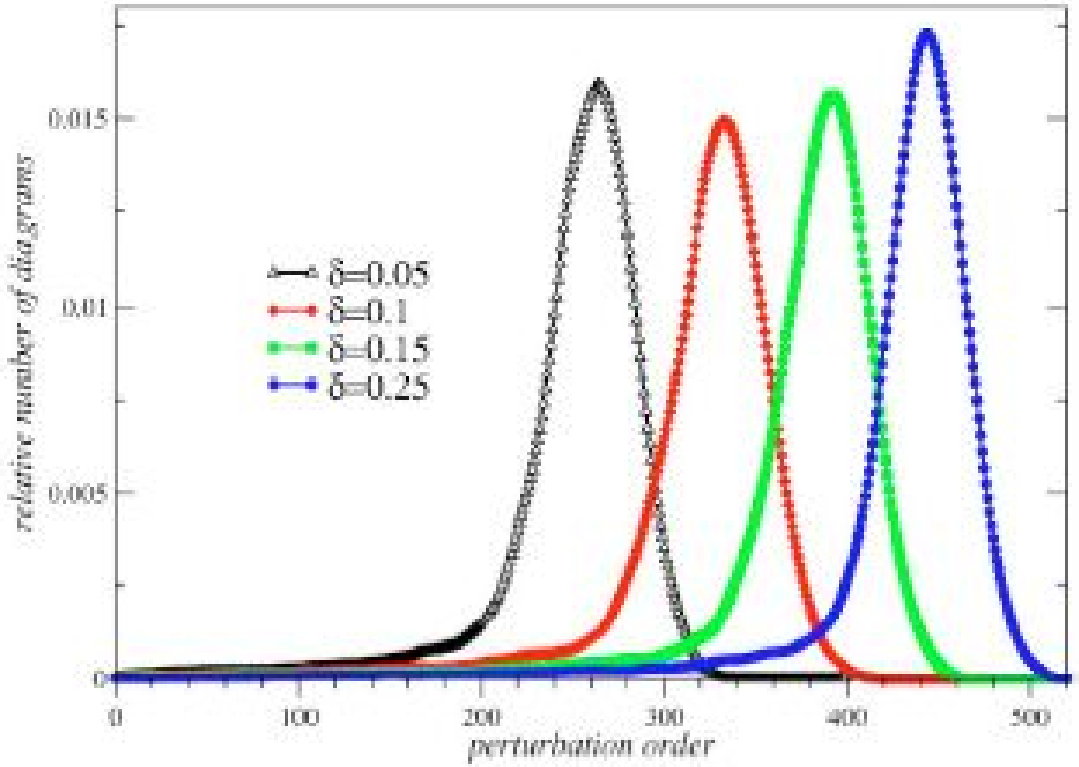

FIG. 1. (Color online) The perturbation order histogram shows the distribution of the typical perturbation order of the diagrams in the simulation. The histogram is peaked around the typical order, which is related to temperature and kinetic energy by $\langle k \rangle = |E_{kin}|/T$.

One-site partition function

$$Z = \int D[\psi^\dagger \psi] e^{-S_{cluster} - \int_0^\beta d\tau \int_0^\beta d\tau' \sum_{\alpha\alpha'} \psi^\dagger_\alpha(\tau) \Delta_{\alpha\alpha'}(\tau,\tau') \psi_{\alpha'}(\tau')}$$

Expansion in hybridization

$$Z = \int D[\psi^\dagger \psi] e^{-S_{cluster}} \sum_k \frac{1}{k!} \left[\sum_{\alpha\alpha'} \int_0^\beta d\tau \int_0^\beta d\tau' \psi_{\alpha'}(\tau') \psi^\dagger_\alpha(\tau) \Delta_{\alpha\alpha'}(\tau,\tau') \right]^k$$

$$Z = \int D[\psi^\dagger \psi] e^{-S_{cluster}} \sum_k \frac{1}{k!} \int_0^\beta \prod_{i=1}^k d\tau_i \int_0^\beta \prod_{i=1}^k d\tau'_i \sum_{\alpha\alpha'} \prod_{i=1}^k \left[\psi_{\alpha'_i}(\tau'_i) \psi^\dagger_{\alpha_i}(\tau_i) \right] \times \prod_{i=1}^k \Delta_{\alpha_i \alpha'_i}(\tau_i, \tau'_i)$$

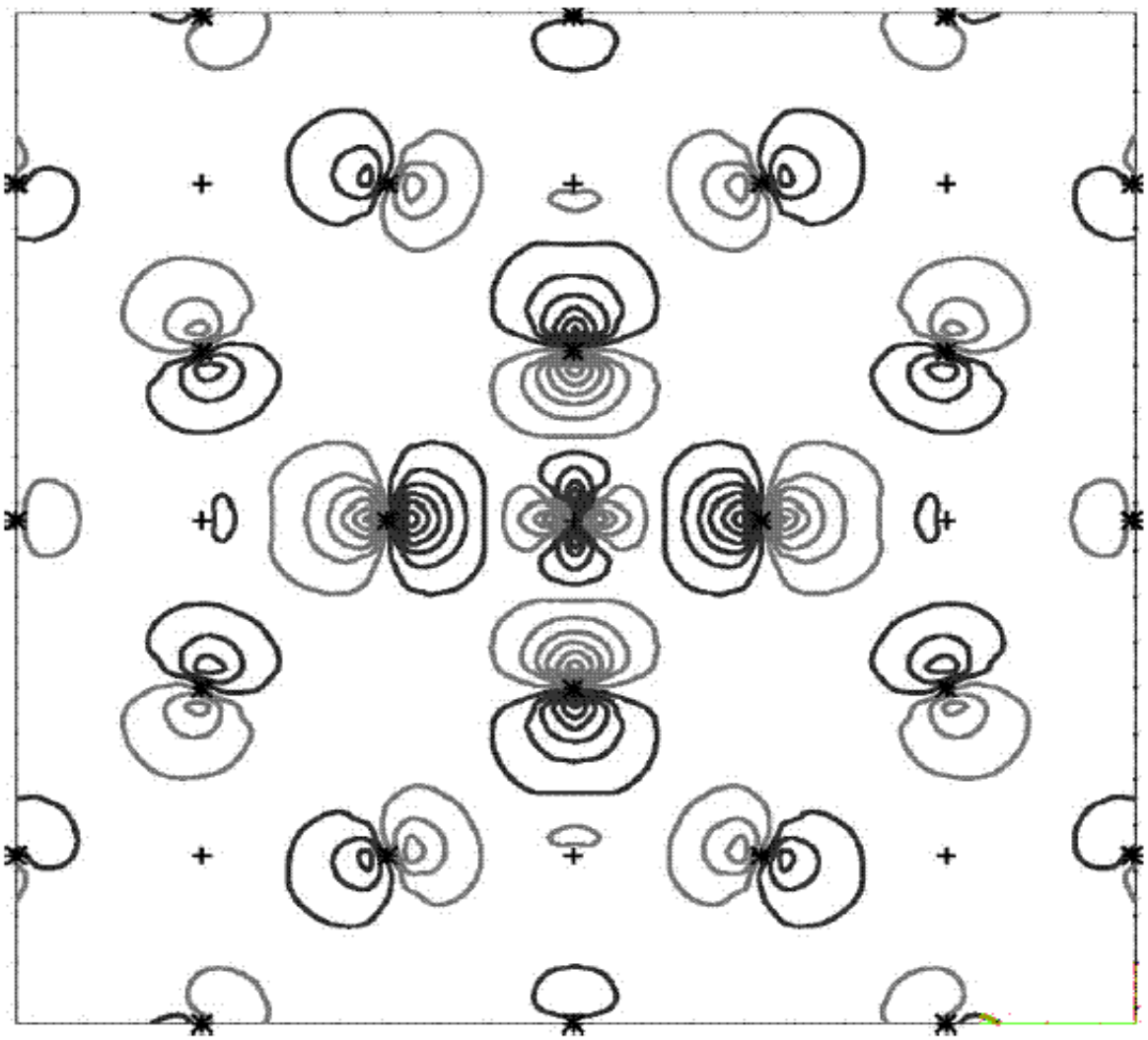

FIG. 1. The Cu $d_{x^2-y^2}$-like LMTO, which describes the (LDA) conduction band of $HgBa_2CuO_4$, plotted in the CuO_2 plane. Cu and O sites are marked by, respectively, + and ※.

Self-energy and effective interaction along imaginary axis